

Supporting Information

Z-scheme Inverse Opal CN/BiOBr Photocatalyst for Highly Efficient Degradation of Antibiotics

Bin Chen^a, Liang Zhou^a, Yunhao Tian^a, Jie Yu^a, Juying Lei^{a,b,*}, Lingzhi Wang^a, Yongdi Liu^{a,b}, Jinlong Zhang^c

^a State Environmental Protection Key Laboratory of Environmental Risk Assessment and Control on Chemical Process, School of Resources and Environmental Engineering, East China University of Science and Technology, 130 Meilong Road, Shanghai 200237, P. R. China. *E-mail: leijuying@ecust.edu.cn.*

^b Shanghai Institute of Pollution Control and Ecological Security, Shanghai, 200092, P.R. China

^c Key Lab for Advanced Materials and Institute of Fine Chemicals, East China University of Science and Technology, 130 Meilong Road, Shanghai 200237, P. R. China.

1. Experimental section

1.1 Preparation of ordered silica PCs

Monodispersed SiO₂ microspheres with a size of ~400 nm were prepared by the Stöber method. Briefly, TEOS (8 mL) was added to ethanol (92 mL) and the mixed solution was stirred to form solution A. Meanwhile, ethanol (56.6 mL), deionized water (29.4 mL) and ammonium hydroxide (14 mL) were added to a round bottom flask (250 mL) to form solution B. Solution A was quickly added to solution B and then the round bottom flask was sealed with a frosted hollow plug. After vigorous stirring for 1 min, the mixture was decelerated to bubble-free stirring. After that, the mixture was kept stirring for 24 h under an oil bath at 25 °C. After the reaction, the prepared silica spheres were washed with water by centrifugation three times to remove unreacted residues. Later, the obtained silica spheres, were dispersed in water with a concentration of 5 wt%, which were then allotted into 10 mL vials. The silica spheres self-assembled to form PCs on the wall of the vials at 110 °C, with little sediment at the bottom.

1.2 Preparation of inverse opal CN (IO CN) and bulk CN

IO CN was prepared based on the previous literature¹. Dicyandiamide (DCDA) (0.6 g) was mixed with silica PCs (1.0 g), and calcined in Ar at 520 °C with a ramp of 2 °C·min⁻¹ for 2 h. Afterward, the product was further heated to 550 °C with a ramp of 4 °C min⁻¹ and kept at 550 °C for another 2 h. The as-obtained product was etched using 4 M NH₄HF₂ aqueous solution for 48 h to remove the silica templates completely, washed with deionized water several times and dried at 60 °C in a vacuum drying oven overnight. The obtained sample was designated as IO CN.

Bulk CN without inverse opal structure was prepared by directly calcining DCDA in air. The temperature program is the same as that of IO CN.

1.3 Preparation of inverse opal CN/BiOBr (IO CN/BiOBr), bulk CN/BiOBr and pure BiOBr

Concretely, 0.0796 g Bi(NO₃)₃·5H₂O and 0.0195 g KBr were firstly dissolved in ethylene glycol to form solution A. Meanwhile, 0.2 g IO CN in distilled water (100 mL) was sonicated for 15 min to form suspension B. Then solution A was added into suspension B under vigorous stirring. Next, the resulting mixture was refluxed in an oil bath at 80 °C under vigorous stirring for 2 h. The products were centrifuged and washed several times with distilled water and absolute ethanol. Finally, the samples were dried overnight at 70 °C. For comparison, bulk CN/BiOBr was prepared by the method similar to that of IO CN/BiOBr and pure BiOBr was also prepared by the same procedure in the absence of IO CN.

2. Characterization

The crystal structure of the samples was investigated using an X-ray diffractometer (XRD, Rigaku D/max 2550 VB/PC) with Cu K α radiation, recorded with 2 θ ranging from 5° to 80°. The morphology of the samples were observed by scanning electron microscopy (SEM, NOVA Nano SEM450). Field emission scanning electron microscope (FESEM) images were acquired using a

Hitachi S-4800 FESEM. High-resolution transmission electron microscopy (HRTEM) images were collected with a JEOL JEM-2100 electron microscope. Surface area measurements and porosity analysis were performed on Micromeritics ASAP 2020 surface area with degassing conditions of 300 °C and 8 h heating. Pore distributions and pore volume were calculated using the adsorption branch of the N₂ isotherms based on the BJH model. The Brunauer–Emmett–Teller specific surface area (BET) was determined by N₂ physisorption using a Micromeritics ASAP 2020 automated system. Chemical compositions of the samples were analyzed using X-ray photoelectrospectroscopy (XPS) (Thermo Scientific ESCALAB 250Xi). All the binding energies were calibrated to the C 1s peak (284.6 eV) arising from the adventitious carbon. UV-Visible absorption spectroscopy tested solid and liquid samples by using an ultraviolet-visible spectrophotometer (UV-2540, Shimadzu, Japan), where a solid sample was tested using BaSO₄ as a reference. The fluorescence test uses a fluorescence spectrophotometer (PTIQM-4) with an excitation wavelength of 360 nm. The time-resolved fluorescence attenuation profile was tested with a fluorescence spectrophotometer (FLS 980) with an excitation wavelength of 470 nm. Electron spin resonance (ESR) signals were recorded on a Bruker EMX 8/2.7 spectrometer at room temperature (298 K). The spectra were obtained using the frequency of 9.883 GHz and 3520 G central magnetic field. Photoelectrochemical tests such as electrochemical impedance (EIS), photocurrent test (POL) and Mottshot base curves were performed using a CHI 660D electrochemical workstation. The details are provided as follow.

3. Electrochemical measurements

The electrochemical measurement was performed on an electrochemical analyzer (Zahner, Zennium) at room temperature. The standard three-electrode system was composed of a working electrode, a Pt wire counter electrode and a saturated calomel reference electrode. The working electrode was prepared by depositing a sample film on a F-doped SnO₂-Coated (FTO) glass. A 5-mg sample was dissolved in 0.5 mL of ethanol, and then 20 μL of solution was dropped on the FTO glass within an area of 1 cm² and dried at room temperature. The transient photocurrent response of the different samples was determined in a 0.5 M Na₂SO₄ aqueous solution under irradiation of a 300 W Xenon lamp without the filter. The electrochemical impedance of the different samples was determined in a mixture including 25 mM K₃[Fe(CN)₆], 25 mM K₄Fe(CN)₆ and 0.1 M KCl.

4. Photocatalytic experiments

In a typical experiment, 0.05 g of as-prepared samples were dispersed into 50 mL of 10 mg/L LVX solution for 20 min in the dark to ensure the adsorption equilibrium of LVX. Subsequently, the suspensions were exposed to visible light irradiation using a 300 W Xenon lamp with a 420 nm cutoff filter. At a given interval (10 min) during visible light exposure, a certain amount of suspension was taken out and filtered using a 0.45 μm Millipore filter to remove photocatalysts before analysis. The LVX concentration of leachate was detected via HPLC (Shimadzu LC-20AD, Japan) at 8 min interval at its characteristic absorption wavelength of 294 nm.

For the degradation of RhB, 0.05 g of as-prepared samples were added into 50 mL of 20 mg/L RhB aqueous solution. Then the suspension was stirred in the dark for 20 min to achieve the adsorption–desorption equilibrium prior to visible light irradiation. The concentration changes of RhB were monitored by measuring the UV–vis absorption of the suspensions at 10 min interval. During irradiation, a certain amount of the suspension was taken out and centrifuged (12,000 rpm,

10 min) to remove the photocatalyst before measurement. The absorbance of RhB at 553 nm was used to determine its concentration by a Shimadzu-UV 2450 UV-vis spectrophotometer.

5. Active species trapping experiments

In order to detect which active species is mainer for the photocatalytic reaction, TEOA (1mM), BQ (1mM), and TBA (1mM) were respectively used as the scavengers for h^+ , $\bullet O_2^-$ and $\bullet OH$. The experiments were similar to the photocatalytic experiments.

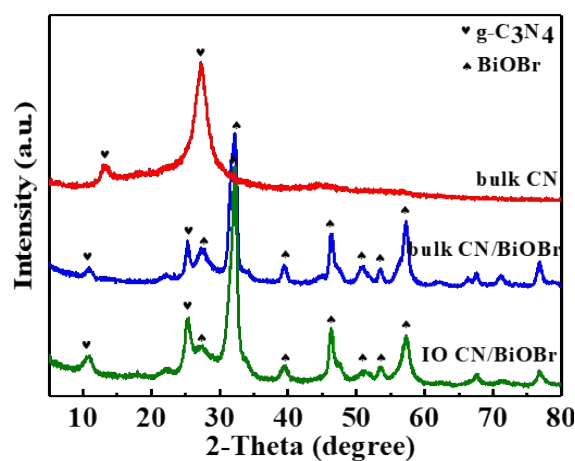


Fig. S1. XRD patterns of bulk CN, bulk CN/BiOBr and IO CN/BiOBr

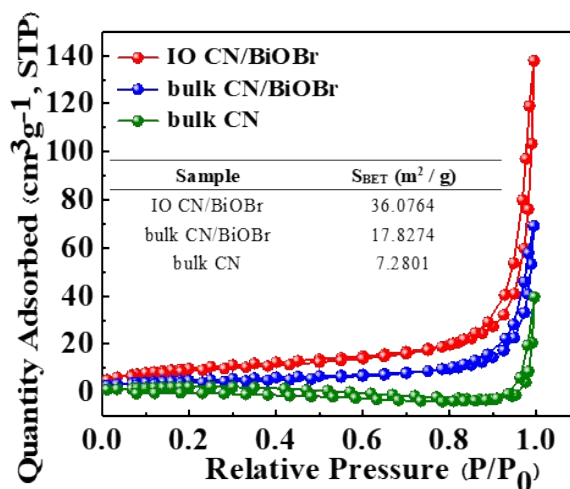


Fig. S2. Nitrogen adsorption-desorption isotherms of IO CN/BiOBr, bulk CN/BiOBr and bulk CN (inserted is the corresponding BET surface area)

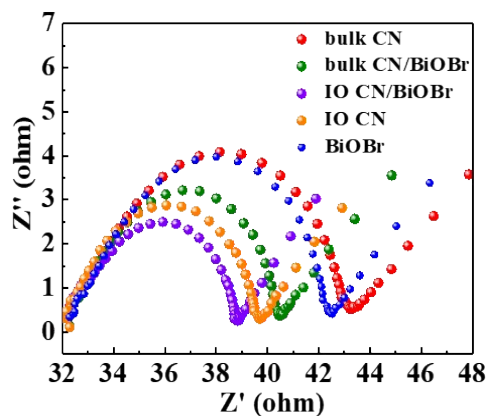


Fig. S3. EIS Nyquist plots of different photocatalysts

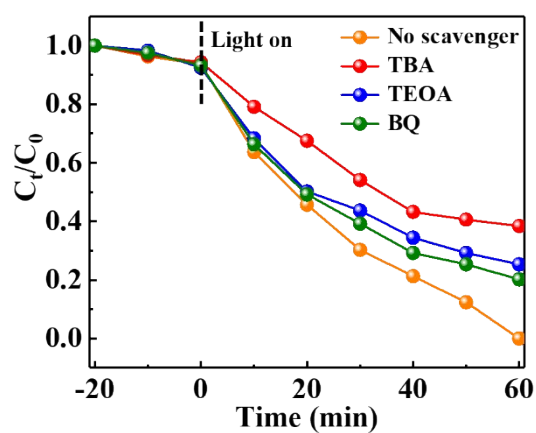


Fig. S4. Effects of different scavengers on the degradation efficiency of LVX over IO CN/BiOBr

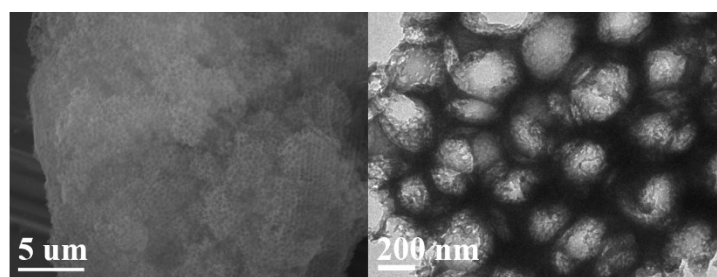


Fig. S5. (A) SEM image of IO CN/BiOBr after the 5th run cycle photocatalytic experiment and (B) TEM image of IO CN/BiOBr after the 5th run cycle photocatalytic experiment

References

1. L. Sun, M. Yang, J. Huang, D. Yu, W. Hong and X. Chen, *Adv. Funct. Mater.*, 2016, **26**, 4943-4950.